Journal of Pharmaceutical and Biomedical Analysis 108 (2015) 78–85

Contents lists available at ScienceDirect

Journal of Pharmaceutical and Biomedical Analysis

journal homepage: www.elsevier.com/locate/jpba

Non-linear effects in quantitative 2D NMR of polysaccharides: Pitfalls and how to avoid them

Estelle Martineau[a,b], Kamel El Khantache[a,b], Marion Pupier[c,1], Patricia Sepulcri[c], Serge Akoka[a], Patrick Giraudeau[a,d,*]

[a] EBSI Team, Chimie et Interdisciplinarité: Synthèse, Analyse, Modélisation (CEISAM), Université de Nantes, CNRS, UMR 6230, LUNAM Université, France
[b] Spectromaîtrise, CAPACITÉS SAS, 26 Bd Vincent Gâche, 44200 Nantes, France
[c] Sanofi Pasteur, Analytical Research Department – CBB, Campus Mérieux – 1541, Avenue Marcel Mérieux 69280 Marcy l'étoile, France
[d] Institut Universitaire de France, 1 rue Descartes, 75005 Paris Cedex 5, France

ARTICLE INFO

Article history:
Received 8 December 2014
Received in revised form 26 January 2015
Accepted 30 January 2015
Available online 7 February 2015

Keywords:
Nuclear magnetic resonance
Quantitative analysis
2D NMR
Polysaccharides
Standard additions

ABSTRACT

Quantitative 2D NMR is a powerful analytical tool which is widely used to determine the concentration of small molecules in complex samples. Due to the site-specific response of the 2D NMR signal, the determination of absolute concentrations requires the use of a calibration or standard addition approach, where the analyte acts as its own reference. Standard addition methods, where the targeted sample is gradually spiked with known amounts of the targeted analyte, are particularly well-suited for quantitative 2D NMR of small molecules. This paper explores the potential of such quantitative 2D NMR approaches for the quantitative analysis of a high molecular weight polysaccharide. The results highlight that the standard addition method leads to a strong under-estimation of the target concentration, whatever the 2D NMR pulse sequence. Diffusion measurements show that a change in the macromolecular organization of the studied polysaccharide is the most probable hypothesis to explain the non-linear evolution of the 2D NMR signal with concentration. In spite of this non-linearity – the detailed explanation of which is out of the scope of this paper – we demonstrate that accurate quantitative results can still be obtained provided that an external calibration is performed with a wide range of concentrations surrounding the target value. This study opens the way to a number of studies where 2D NMR is needed for the quantitative analysis of macromolecules.

1. Introduction

Nuclear magnetic resonance (NMR) is one of the most versatile analytical techniques, and its quantitative potential is widely recognized. Liquid-state quantitative NMR has been used for decades in a large range of application fields, such as pharmaceutical analysis, natural products, *in vivo* spectroscopy and metabolomics. A large majority of quantitative NMR studies have taken advantage of the high sensitivity of the ^{1}H nuclei; unfortunately ^{1}H NMR is often hampered by the high degree of overlap characterizing 1D spectra, particularly when the analytes are studied in complex environments. Several solutions have been considered to overcome this overlap problem, such as the use of spectral deconvolution procedures or the use of other nuclei with wider spectral ranges such as ^{13}C [1] or ^{15}N [2]. Another appealing solution is to rely on two-dimensional NMR, a technique proposed by Jeener in 1971 and applied for decades as a routine tool for the elucidation of small organic molecules or macromolecular structures [3,4]. From the quantitative point of view, 2D NMR has the high advantage of offering a much better discrimination of resonances than 1D NMR, as the peaks are spread along an additional orthogonal dimension. The use of 2D NMR for quantitative analysis has been particularly expanding during the last decade [5–11], a late development which is explained by two main drawbacks. The first one is the long experiment duration inherent to the time incrementation procedure associated with the acquisition of the indirect dimension. Typical 2D NMR experiments last between a few tens of minutes to a few hours, which not only overloads the spectrometer schedules, but also significantly affects the repeatability of quantitative

* Corresponding author at: Chimie et Interdisciplinarité: Synthèse, Analyse, Modélisation (CEISAM), UMR 6230, Faculté des Sciences, BP 92208, 2 rue de la Houssinière, F-44322 Nantes Cedex 03, France. Tel.: +33 2 51 12 57 09; fax: +33 2 51 12 57 12.
E-mail address: patrick.giraudeau@univ-nantes.fr (P. Giraudeau).
[1] Present address: Department of Organic Chemistry, University of Geneva, 30 Quai E. Ansermet, 1211 Geneva 4, Switzerland.

http://dx.doi.org/10.1016/j.jpba.2015.01.056
0731-7085/

measurements, leading to a relatively poor precision [11,12]. It also makes it difficult to study samples whose composition evolves in the course of time under the effect of kinetic or dynamic processes. Fortunately, a number of strategies have been proposed to reduce the duration of quantitative 2D NMR experiments, from the careful optimization of acquisition and processing parameters [7,8,13,14] or the use of covariance spectroscopy [15,16] to the use of different sampling strategies such as ultrafast 2D NMR [12,17].

The second main challenge of quantitative 2D NMR is that – contrary to one pulse 1D NMR – the coefficient of proportionality k between the 2D peak volume and the concentration is highly site-specific, as it depends on several peak-dependant factors (transverse relaxation times, J-couplings and pulse sequence delays). Because this dependence is *a priori* not known, it is necessary to find a way to determine – or to get rid of – the proportionality constant k for each peak, in order to reach a high trueness in the determination of the analyte concentrations. Three families of approaches have been described to reach this goal. The first one consists in modifying the NMR experiment itself to remove the dependence of k on the different factors mentioned above, so that the peak volume is not site-specific anymore [18]. A second strategy consists in determining, for each peak, the exact value of k, based on theoretical considerations [19]. A last family of approaches also determines the different k values, but by relying on more classical analytical approaches such as calibration or standard additions [7,10]. As recently described [11], so far only the last family of approaches has succeeded in reaching a high precision, and has become applicable in routine. Combined to fast acquisition protocols, calibration and standard addition methods have been particularly successful in determining the concentration of small metabolites in complex mixtures such as plant tissue extracts [7], cancer cell extracts [10,17], biological fluids [20,21], *etc.* An accuracy of a few percent was generally reported for acquisitions performed within reasonable experiment times.

While they may seem relatively similar, calibration and standard addition methods are relatively different in that the first one can be seen as an external reference, while the second one acts as an internal reference [22]. The external calibration strategy consists in recording NMR spectra on a series of standards in different concentrations, plotting their 2D NMR peak volumes *versus* their concentrations, and then using the resulting curve to determine the concentration of the unknown sample. This approach is well adapted to the simultaneous quantification of multiple compounds, however it may suffer from the differences that occur between the model samples used for calibration and the complex sample in which the quantification is performed. As a consequence, the NMR response of the external standards may differ from the one of the sample of interest, which affects the trueness of the analytical method. On the contrary, in the standard addition approach, the target analytes are acting as their own reference, and the whole procedure is carried out within the same NMR tube, thus avoiding the inter-sample variation drawback of the external calibration approach. Here, known amounts of the target analyte (or mixture of analytes) are gradually spiked to the analyzed sample. For each analyte whose concentration needs to be determined, a standard addition curve is fitted by the linear regression equation: $V = a \cdot [c] + b$, where V represents the 2D peak volume and $[c]$ the concentration of the analyte in the sample. The initial concentration of the analyte in the sample is calculated by the b/a ratio, where a is the slope and b the y-intercept of the linear regression curve [23]. Recently, we demonstrated that a high trueness could be reached by coupling a standard addition method to a quantitative 2D NMR approach [10,17]. However, only small molecules were targeted in these recent applications.

Therefore, the goal of this paper is to determine whether these recent quantitative 2D NMR approaches can be efficiently applied to the accurate quantification of bigger molecules. Polysaccharides have been chosen for this study, as they play a major role in many biological systems and processes of all kingdoms (Animalia, Plantae, Fungi, Protista, Archaea, and Bacteria) without forgetting viruses. Largely used in many industries (food, biomaterials, cosmetics, etc.) [24,25] for their sweetening or thickening properties or for their resistance, polysaccharides are also used in the pharmaceutical industry [26,27] for therapeutic (drugs) and prophylactic purposes (vaccines) [28]. Polysaccharides can be active components, adjuvants but also unwanted residuals. Therefore, being able to quantify them in complex solutions – such as intermediates of manufacturing processes or vaccine doses – is important for understanding and developing the associated products and processes. As quantification can be really challenging in such complex mixtures by the classical methods or by 1D NMR, the 2D NMR approach is a major potential alternative method. The potential of 2D NMR to determine the composition of polysaccharides was recently highlighted, but it was never used for concentration determination purposes [29,30]. In this paper, we explore the potential of quantitative 2D NMR experiments combined with a standard addition procedure to determine the concentration of a model polysaccharide. Unexpected results are described and analyzed in order to propose a reliable protocol for quantitative 2D NMR of such macromolecules.

2. Results and discussion

2.1. Model molecule

The model molecule chosen for this study is the capsular polysaccharide PRP (Poly(ribosyl-Ribitol-Phosphate)) produced by *Haemophilus influenzae* type b (Hib) responsible of serious invasive diseases such as meningitis in infants. PRP is the protective immunogen used in commercially available anti-Hib vaccines. It is a linear polymer of the repeating unit [3)-β-D-Ribf-(1 → 1)-D-ribitol-5-*P*-(O →]$_n$ [31]. Fig. 1 shows the 1D and 2D spectra of PRP which were recorded on a 500 MHz spectrometer equipped with a cryoprobe. The structure of PRP is represented in Fig. 1 (a), together with the corresponding 1D spectrum. The four cyclic protons (H_1, H_2, H_3 and H_4) are clearly identified [32–35] and are used for quantification throughout this study. They have been chosen because they correspond to well-separated peaks on the 1D spectrum, therefore they can be used to compare the quantitative results obtained by 2D *versus* 1D NMR experiments. These protons also give rise to well identified correlation peaks on 2D spectra. Fig. 1 (b–d) presents representative examples of 2D experiments which have been used recently in the literature for quantitative analysis: zero-quantum filtered total correlation spectroscopy (ZQF-TOCSY) [9,36], ^{1}H Incredible Natural Abundance DoublE QUAntum Transfer Experiment (INADEQUATE) [8,10] and ^{1}H–^{13}C Heteronuclear Single Quantum Coherence (HSQC) [7,37]. Note that the INADEQUATE experiment is generally used to establish ^{13}C–^{13}C connectivities, but that its ^{1}H–^{1}H version is also a powerful analytical tool to simplify the homonuclear 2D spectra of complex mixtures [8,10], an approach similar to the Maximum Quantum strategy described by Caldarelli and co-workers [38]. The three experiments cited above have been characterized by excellent analytical performances (repeatability and linearity) on small molecules, and detailed information about the corresponding experiments can be found in the references mentioned above. The signal attributions are also reported on the 2D spectra; for example, in Fig. 1 (b) and (c), H_1/H_2 symbolizes the correlation peak between H_1 (F_2 dimension) and H_2 (F_1 dimension). Likewise, $H_3/(H_2 + H_4)$ represents the correlation peak between H_3 (F_2 dimension) and H_2 and H_4 (F_1 dimension): these two protons

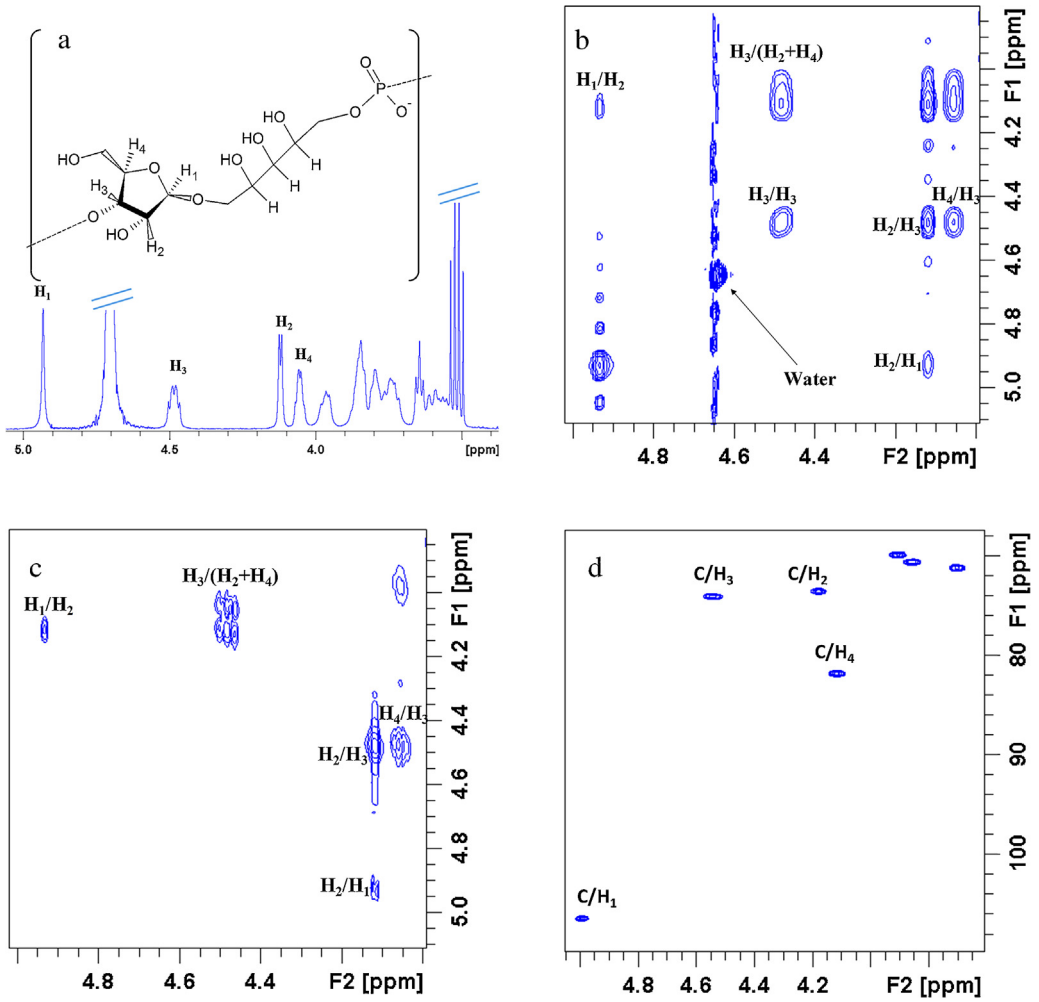

Fig. 1. Different NMR spectra of a 5.51 mmol L^{-1} Poly(ribosyl-Ribitol-Phosphate) (PRP) sample in D_2O, recorded at 500 MHz with a cryoprobe. (a) One-dimensional ^1H NMR spectrum and molecular structure of the PRP; (b) Two-dimensional ZQF-TOCSY spectrum; (c) Two-dimensional ^1H INADEQUATE spectrum; (d) Two-dimensional ^1H–^{13}C HSQC spectrum.

cannot be discriminated due to an overlap along the F_1 dimension. Correlation peaks between protons and the corresponding carbons are also indicated on the HSQC spectrum (Fig. 1(d)).

2.2. Standard additions

The initial aim of this work was to determine the concentration of PRP in a model solution S1 (target concentration: 5.51 mmol L^{-1}) by relying on a standard addition procedure as described in the introduction, *i.e.* the unknown concentration is determined by adding known amounts of PRP to the initial sample. However, for the analytical study described below, which required performing multiple experiments for each added concentration, we actually prepared three additional samples (S2, S3 and S4) mimicking those that would have been obtained by spiking the sample S1 with known amounts of PRP. Thanks to this procedure, we could avoid preparing fresh samples between each series of acquisitions, and all the acquisition methods were compared on the same samples, thus excluding errors that could arise from the sample preparation procedure. For each sample, 1D and 2D NMR signals were measured on each spectrum for all the integration sites described in Fig. 1. The NMR signal was then plotted as a function of the added concentration, and the equation of the linear regression curve led to the determination of the "unknown" concentration. Fig. 2 represents the standard addition curves (normalized to the signal measured for S1) obtained by 1D ^1H NMR and by three different 2D NMR experiments. The concentration determined by the standard addition procedure is given by the intersection of the linear regression curve with the horizontal axis (empty circles). It clearly appears that the concentration determined by 1D NMR is very close to the target concentration. On the contrary, the concentration determined by the 2D NMR experiments is systematically underestimated, whatever the pulse sequence used. Similar results are obtained whatever the peak chosen for quantification, as shown by the quantification results in Table 1, which also includes results obtained with two other pulse sequences: ^1H Correlation Spectroscopy (COSY) and ^1H-^{31}P HSQC. Even though the determination coefficient of the regression curve is excellent for all experiments and all signals, only 1D NMR leads to acceptable quantification results (error lower than 7%), while the deviation to the target concentration obtained by 2D NMR is always higher than 25%. These results clearly indicate that the standard addition approach is not suitable to quantify PRP by 2D NMR, contrary to what we recently described for small molecules [8,17]. Several hypotheses have been made in order to understand why the concentration was underestimated by 2D NMR.

2.3. Non-linear evolution of the 2D NMR signal

First of all, Table 1 demonstrates that the poor accuracy does not depend on the pulse sequence used: indeed, for each 2D sequence

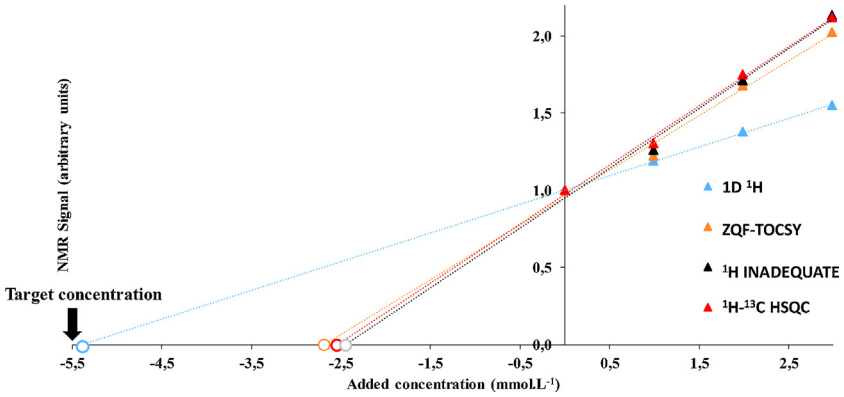

Fig. 2. Standard addition curves of the PRP in D_2O for different NMR experiments performed at 500 MHz with a cryoprobe. Filled triangles represent the signal measured on the spectra recorded on solutions S1 to S4, while empty circles correspond to the extrapolation of the linear regression curve at $y = 0$, giving access to the concentration of the S1 solution. The target concentration is also indicated. The following signals were used for plotting these curves: H_1 for 1D NMR, H_1/H_2 for ZQF-TOCSY, H_4/H_3 for ^{1}H INADEQUATE and C/H_2 for ^{1}H–^{13}C HSQC. Similar results are obtained with other signals, as shown in Table 1. All the signals were normalized to 1 for an added concentration equal to zero.

applied, the targeted concentration is always underestimated by the standard addition procedure. After this initial observation, we first suspected the presence of radiation damping (RD) but this hypothesis was invalidated by additional measurements performed in a less sensitive hardware configuration, where similar results were obtained (Supporting Information Table S1).

Another possible source of error could arise from longitudinal relaxation times (T_1). It has been shown that when standard additions or calibration curves are used, it is possible to work under partial saturation conditions, provided that T_1s do not vary over the studied concentration range [8,17]. In order to ensure that it was not the case here, we measured the T_1s of the different molecular sites on the initial solution and after the last standard addition.

Table 1
Quantification results for the PRP sample in D_2O (target concentration = 5.51 mmol L^{-1}) obtained with a standard addition approach performed with different NMR pulse sequences on a 500 MHz spectrometer with a cryoprobe. The accuracy corresponds to the deviation to the target concentration.

Pulse sequence	Peak	r^2	Accuracy (%)
1D ^{1}H	H_1	0.9992	−2
	H_2	0.8891	5
	H_3	0.9961	−7
	H_4	0.9872	0
ZQF-TOCSY	H_1/H_2	0.9887	−49
	H_2/H_1	0.9995	−46
	$H_3/(H_2 + H_4)$	0.9995	−39
	H_3/H_3	0.9995	−42
	H_4/H_3	0.9989	−27
	H_2/H_3	0.9980	−46
COSY	H_1/H_2	0.9919	−60
	H_2/H_1	0.9773	−65
	H_3/H_4	0.9913	−52
	H_3/H_2	0.9889	−58
	H_3/H_3	0.9941	−38
	H_4/H_3	0.9975	−45
	H_2/H_3	0.9889	−57
^{1}H INADEQUATE	H_1/H_2	0.9643	−65
	H_2/H_1	0.9686	−64
	$H_3/(H_2 + H_4)$	0.9818	−59
	H_4/H_3	0.9886	−56
	H_2/H_3	0.9870	−57
HSQC ^{1}H – ^{13}C	C/H_1	0.9985	−42
	C/H_3	0.9991	−44
	C/H_2	0.9952	−54
	C/H_4	0.9972	−26
HSQC ^{1}H – ^{31}P	H_3/P	0.9720	−58

The results (Supporting Information Table S2) show that the T_1s do not vary significantly over the concentration range. Therefore, partial saturation effects cannot explain the high quantification errors described above. Moreover, such effects would probably have biased the results obtained by 1D NMR as well, which was obviously not the case.

Based on these unsuccessful attempts, we decided to observe the evolution of the 2D NMR signal over a larger concentration range, in order to detect possible non-linear effects. We prepared five additional samples with PRP concentrations lower than the one of the S1 solution, and we measured the NMR signals obtained with several pulse sequences. The NMR signals were then plotted *versus* the real concentration of PRP. From the corresponding calibration curves (Fig. 3), the non-linear evolution of the 2D NMR signal is blindingly obvious, whatever the pulse sequence. The same result was observed for all signals of the 2D spectra, which explains why the concentration of S1 obtained with the standard addition procedure was systematically underestimated. This result is contradictory with those obtained on small molecules, where a high linearity was systematically reported for large concentration ranges [7,8,10,17,20,21]. The main consequence is that the quantification of macromolecules such as PRP by 2D NMR cannot be performed by a standard addition procedure, but requires an external calibration approach with a concentration range including the target concentration. Of course, such calibration curves cannot be fitted by a linear regression model, but a good correlation can be obtained with a non-linear regression. In order to evaluate the performance of this approach, the point corresponding to the target solution S1 was removed from the calibration graph, and the remaining points were fitted by a polynomial equation -a polynomial of degree 4 led to the best fit. There is actually no physical meaning for this dependence, which is only the result of the best polynomial fit that could adjust the experimental points. Closely looking at the curves in Fig. 3, a bi-linear fit would also be an option which would be coherent with a change in the macromolecular organization with concentration, as described in Section 2.4. This bi-linear fit was added on the curves, still it fails to accurately predict the peak volumes in the middle of the concentration range, where our target concentration stands. We therefore suggest to use the polynomial fit for the determination of concentration.

The quantification results are presented in Table 2. We can observe that for each sequence and each integration site, the deviation to the target concentration is lower than 5%, which demonstrates the excellent accuracy of the calibration approach. Moreover, the very high determination coefficients r^2 obtained for

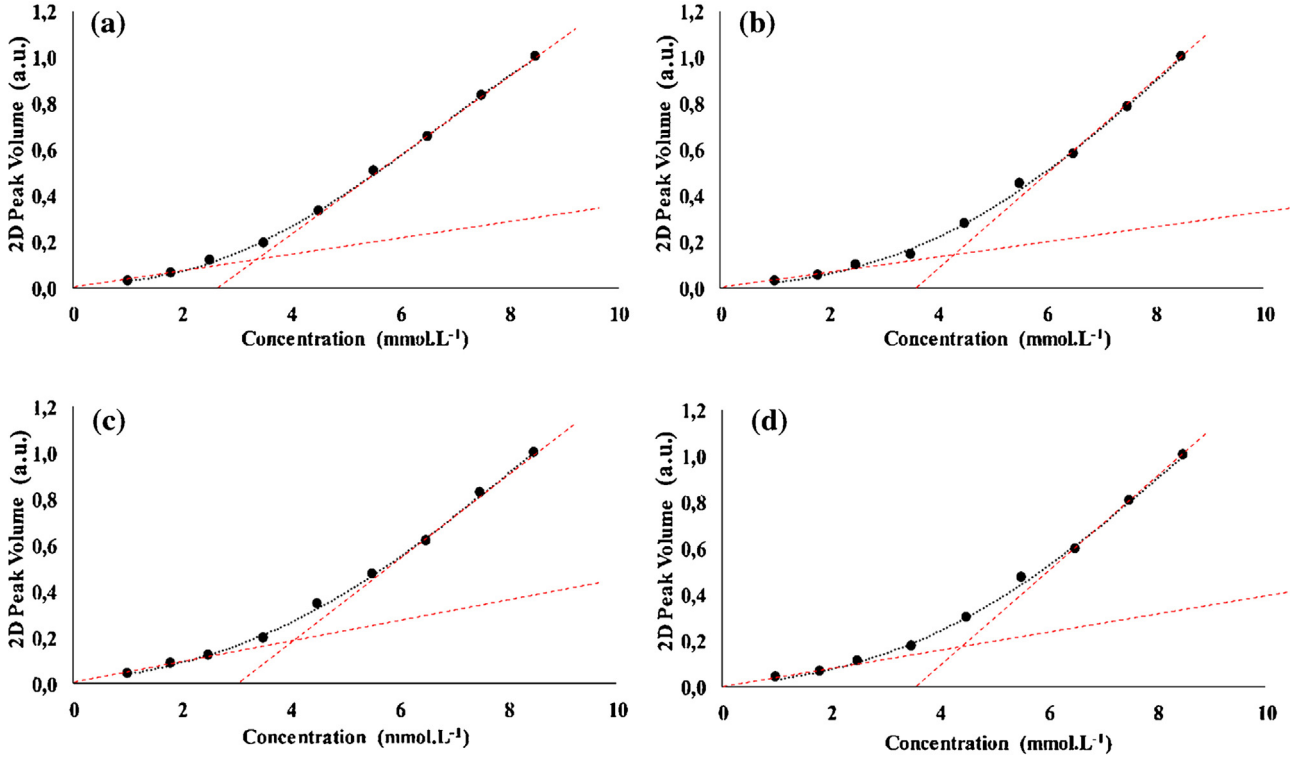

Fig. 3. Calibration curves of the PRP in D_2O for different NMR experiments performed at 500 MHz with a cryoprobe. The following signals were used for plotting these curves: H_2/H_1 for ZQF-TOCSY (a), H_3/H_2 for COSY (b), C/H_2 for $^1H–^{13}C$ HSQC (c) and H_4/H_3 peak for ^1H INADEQUATE (d). Similar results are obtained with other signals and pulse sequences. All the signals were normalized to 1 for the most concentrated sample. The best polynomial fit (black dotted lines) was obtained with a polynomial of degree 4. The apparent bi-linearity of the curves is also highlighted (red dashed lines).

each site confirm the quality of the regression. The external calibration is consequently the best way to accurately determine the concentration of such macromolecular samples. Compared to the standard addition procedure, this strategy presents some drawbacks, in particular when the target molecule needs to be quantified in a complex mixture – which is almost always the case when the use of quantitative 2D NMR is considered. In this case, the experimentalist must ensure that the calibration samples are as close as possible to the complex sample (particularly in terms of pH) so that the 2D peak volume evolution in the calibration samples is representative of those measured in the complex sample. Still, these results demonstrate that the external calibration procedure is much more adapted than standard additions for the accurate quantification of this high-molecular weight polysaccharide.

Table 2
Quantification results for the PRP sample in D_2O (target concentration = 5.51 mmol L^{-1}) obtained with a calibration approach performed with different NMR pulse sequences on a 500 MHz spectrometer with a cryoprobe. The accuracy corresponds to the deviation to the target concentration.

Pulse sequence	Peak	r^2	Accuracy (%)
ZQF-TOCSY	H_1/H_2	0.9992	7
	H_2/H_1	0.9998	1
	$H_3/(H_2+H_4)$	0.9997	1
	H_3/H_3	0.9996	1
	H_4/H_3	0.9997	−5
	H_2/H_3	0.9993	1
COSY	H_1/H_2	0.9991	5
	H_2/H_1	0.9989	6
	H_3/H_4	0.9996	5
	H_3/H_2	0.9995	5
	H_3/H_3	0.9998	4
	H_4/H_3	0.9996	−2
	H_2/H_3	0.9995	−3
^1H INADEQUATE	H_1/H_2	0.9975	0
	H_2/H_1	0.9972	−1
	$H_3/(H_2+H_4)$	0.9988	−2
	H_4/H_3	0.9988	−2
	H_2/H_3	0.9990	−2
HSQC $^1H–^{13}C$	C/H_1	0.9999	5
	C/H_3	0.9997	1
	C/H_2	0.9999	3
	C/H_4	0.9997	−3
HSQC $^1H–^{31}P$	H_3/P	0.9989	−8

2.4. Possible origin of non-linear effects

The last part of this manuscript discusses some hypotheses that could explain the origin of the non-linear effects observed above, considering that such effects were observed in 2D but not in 1D NMR. Because of the high molecular weight of the PRP, we suspected that a change in nuclear Overhauser effect (NOE) with concentration could be at the source of this non-linearity. Contrary to the one-pulse 1D experiment where the NOE does not impact the peak area, 2D experiments are multi-pulse, and as the spin system is out of equilibrium, NOE can impact the peak volumes during the different evolution delays of the 2D pulse sequence. In order to assess the impact of homonuclear NOE as a function of concentration, we performed 2D NOESY (NOE Spectroscopy) experiments for several of our samples at different concentrations. Strong correlation peaks were observed for all protons, with the same sign as the diagonal peaks, which is expected in the case of macromolecules with long correlation times. The correlation peak volumes were normalized by the volume of the corresponding diagonal peaks. These relative peak volumes were plotted against concentration, as shown in Fig. 4 for the H_2 proton (similar curves were obtained for all signals – results not shown). Fig. 4 shows a non-linear decrease of NOE with the concentration, which can be correlated with the

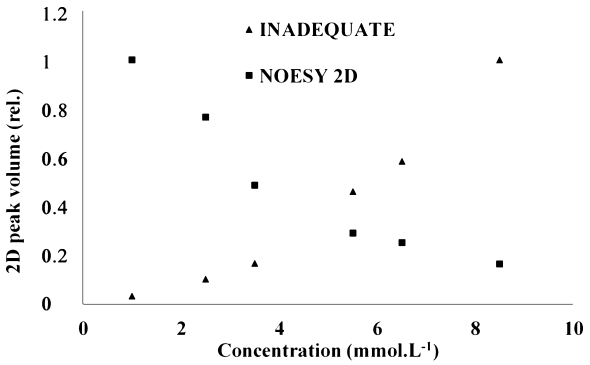

Fig. 4. Relative evolution of the sum of the 2D NOESY cross-peak volumes involving the H_2 proton (normalized by the corresponding diagonal peak volume). For the sake of comparison, the evolution of the H_2/H_3 peak volume for the ^1H INADEQUATE experiment is also plotted. The data were obtained on a 500 MHz spectrometer equipped with a cryoprobe.

non-linear response of the 2D NMR signal in the experiments described above.

The explanation of this non-linear evolution of NOE is certainly complex, but some hypotheses can be raised to explain it at least partially. In particular, it could be linked to a change in the global mobility of the PRP with concentration. As shown by additional NMR diffusion measurements (Supplementary Fig. S1), the diffusion coefficient of the PRP changes as a function of concentration with a drop in the middle of the concentration range – the diffusion coefficient is divided by a factor 2. Such effect could be in favor of a change in the global molecular tumbling due to a change in the macromolecular organization – such as the formation of aggregates – for concentrations around 4 mmol L^{-1}. While the formation of micelles is likely to occur in such compounds [15], it would have probably led to a more dramatic change in the diffusion coefficient values. The hypothesis of a macroscopic change is further corroborated by an apparent bi-linear evolution of the 2D peak volumes which is highlighted in Fig. 3. This bi-linear evolution could highlight the presence of two distinct macromolecular configurations throughout the studied concentration range.

The hypothesis of a change in the local mobility was also assessed. For that, the ^1H full widths at half height (FWHH, Supplementary Table S3) were measured for different samples over the concentration range, as a marker of change in T_2 relaxation. The FWHH values are characterized by a variation between 0% (for H_2) and 37% (for H_1). These relatively low variations – at least for some of these protons – indicate that the local mobility does not change dramatically, and they are rather unlikely to explain the strong non-linear effects described above: for example, the 2D peak volume of H_2 shows the same non-linear evolution as H_1 with concentration, even though the FWHH of H_2 does not change. Still, the non-linear results presented so far are specific to the protons of the cyclic ribofuranose ring, whose internal mobility is highly constrained. Therefore, additional peak volume determinations were performed from the signals of the more flexible acyclic ribitol residue on the ^1H–^{13}C HSQC spectrum (Supplementary Fig. S2). The results lead to the same non-linear behavior as observed in Fig. 3 c. This result demonstrates that the effect is not related to the internal flexibility of the macromolecule, but rather to a change in the global molecular tumbling change as described above.

A last effect that may complicate even further the interpretation of non-linear NOE effects is the influence of spin diffusion. This phenomenon can take place for molecules with high correlation times such as PRP. In this case, cross relaxation becomes very efficient and leads to ambiguities in the interpretation of NOESY peak volumes, as highlighted by Keeler [39]. Spin-diffusion, which increases with concentration, could therefore reduce the efficiency of the dipolar coupling, thus decreasing the impact of NOE.

These arguments highlight the complexity of the different effects that could explain the non-linear behavior described in this study. Still, the diffusion measurements show that a change in the macromolecular organization of the PRP is the most probable hypothesis to explain the non-linear effects described above. Moreover, additional experiments performed with two different versions of the HSQC pulse sequence (Supplementary Fig. S3), also show that the degree of non-linearity is pulse-sequence dependent. The non-linearity is less pronounced when a more compact pulse sequence is used. This observation is coherent with the hypothesis described above, as changing the number of pulses in the pulse sequence is likely to impact the influence of NOE on 2D peak volumes.

3. Material and methods

3.1. Chemicals

Poly(ribosyl-Ribitol-Phosphate) with sodium as a counter-ion was obtained by bacterial fermentation at Sanofi Pasteur Manufacturing Division, Marcy l'Etoile, France. Deuterium oxide (D_2O; 99.9%D) was purchased from EURISOTOP (www.eurisotop.com). All the concentrations are given relatively to the repeat unit, whose molecular weight is 368 g mol^{-1}, and the apparent size of the PRP is several hundreds of kDa.

3.2. Sample preparation

PRP was diluted in different amounts of D_2O in order to prepare the samples mimicking the standard addition procedure and for the calibration curves. All the samples were homogenized and filtered in a 5 mm NMR tube. Next, the samples were sonicated for 5 min in an ultrasound bath to allow degassing. After this step, a gentle flow of N_2 gas was sent on each sample in order to avoid the increase of residual water.

In the first part of this work, we used a short range of concentrations to mimic the standard addition procedure. Solutions S1–S4 had the following real concentrations in PRP: 5.51; 6.50; 7.50 and 8.49 mmol L^{-1}, corresponding to added concentrations of 0.00; 0.99; 1.99 and 2.98 mmol L^{-1} vis-à-vis the initial solution S1. In the second part of the study, the concentration range was extended by preparing five additional solutions with the following PRP concentrations: 1.00; 1.80; 2.50; 3.50 and 4.50 mmol L^{-1}.

3.3. Spectrometers

The different measurements presented in this paper were performed on three Bruker spectrometers operating under Topspin 2.1. Most of the experiments were recorded at 293 K on a Bruker Avance III 500 MHz spectrometer equipped with a cryogenic $^1H/^{13}C$ probe, at a frequency of 500.13 MHz. To evaluate the effect of radiation damping, additional experiments were performed at 298 K on a Bruker Avance 400 spectrometer, at a frequency of 400.13 MHz with a 5 mm dual+ $^1H/^{13}C$ probe. 2D HSQC ^1H–^{31}P spectra were recorded at 298 K on a Bruker Avance III 400 MHz spectrometer equipped with a BBFO probe, at a frequency of 400.13 MHz.

3.4. Acquisition parameters

All experiments were performed with conventional acquisition parameters. For homonuclear experiments, the residual water

signal was presaturated during the recovery delay, and we verified that the presaturation did not significantly impact the 2D peak volumes and the shape of the calibration and standard addition curves. The repetition time TR (including the acquisition time and the recovery delay) was set to *ca.* 3 s, corresponding to three times the longest T_1. 1D spectra were recorded with eight scans (500 MHz) or 16 scans (400 MHz) and with an 11 ppm spectral width. Homonuclear 2D experiments were recorded with four dummy scans and a number of scans depending on the pulse sequence: one for ZQF-TOCSY, two for COSY and ^{1}H INADEQUATE, and four for NOESY. The spectral width was 6 ppm × 6 ppm, and the number of t_1 increments was set to 128 (ZQF-TOCSY), 256 (NOESY) or 512 (COSY and ^{1}H INADEQUATE). For ZQF-TOCSY, a DIPSI-2 mixing sequence was applied during 80 ms, flanked by adiabatic chirp pulses applied together with gradients, with the same parameters as those described in Ref [9]. ^{1}H–^{13}C HSQC experiments were recorded without water presaturation, with 2 dummy scans, 16 scans, 256 t_1 increment, a 6 ppm width in the ^{1}H dimension and a 80 ppm spectral width in the ^{13}C dimension. The repetition time TR (including the acquisition time and the recovery delay) was set to 2.4 s, and experiments performed with a longer TR (4.8 s) demonstrated that incomplete relaxation was not at the source of the effects observed (Supplementary Fig. S3). The pulse sequence (hsqcedetgp) included an optimized gradient-based coherence-selection scheme. Additional experiments (Supplementary information) with a simpler HSQC experiment (hsqcgpph) were also performed. A GARP ^{13}C decoupling was applied during the ^{1}H acquisition. The INEPT delay was optimized for an average ^{1}H–^{13}C coupling constant of 145 Hz. ^{1}H–^{31}P HSQC experiments were recorded with 4 dummy scans, 64 scans, 32 t_1 increments, a 6 ppm spectral width in the ^{1}H dimension and a 3 ppm spectral width in the ^{31}P dimension. A single correlation peak was detected and used for quantification, thus explaining the low ^{31}P spectral width and the reduced number of t_1 increments. The INEPT delay was optimized for an average ^{1}H–^{31}P coupling constant of 7.6 Hz. A GARP ^{31}P decoupling was applied during the ^{1}H acquisition.

All the experiments used in this study were previously shown to be highly reproducible [10,36,37], therefore the reproducibility was not further assessed in this manuscript. But the fact that a similar non-linearity is obtained with different pulse sequences recorded at different times, emphasizes that the effects observed are not due to repeatability issues.

3.5. Processing parameters

All the spectra were processed using Topspin 3.0. After the acquisition, all the FIDs were weighed by suitably chosen apodization functions: exponential (LB = 0.3 Hz) for 1D and ZQF-TOCSY spectra, sine for COSY spectra, Lorentzian-Gaussian (LB = −1 Hz and GB = 0.15 Hz) for ^{1}H INADEQUATE and NOESY, and sine^2 for ^{1}H–^{13}C HSQC and ^{1}H–^{31}P HSQC. All FIDs were zero-filled twice. The baseline of 1D spectra was manually corrected. For 2D spectra, several baseline corrections were evaluated, but they did not significantly impact the quantitative results. Therefore, no baseline correction was finally applied on 2D spectra.

3.6. Signal integration

1D peak areas and 2D peak volumes were measured using the integration tools available in Topspin 3.0. The integration regions were defined on the most concentrated sample, and chosen so that they do not overlap. They were systematically applied to the spectra of the less concentrated samples. Peak areas or volumes were then exported to Microsoft Excel where the graphs were plotted and the concentrations were calculated.

4. Conclusion

This paper describes a quantitative 2D NMR approach to determine the concentration of polysaccharides in solution. The results described above show that 2D NMR can be used for the accurate quantification of polysaccharides, provided that a calibration procedure is carried out on a range which includes the target concentration. This approach is *a priori* applicable to all commonly used homonuclear or heteronuclear 2D experiments. On the contrary, the standard addition procedure, which is extremely accurate in small molecule studies, cannot be applied here, due to a non-linear evolution of 2D NMR peak volumes as a function of concentration.

These results pave the way toward a number of applications where various macromolecules could be quantified in complex mixtures by 2D NMR. It would also be interesting to determine if the non-linear effects change when the counter-ion is different and if they exist for other polysaccharide structures. Further investigations will consider the application of these methods to determine the concentration of multiple macromolecules in complex mixtures, as well as the use of faster acquisition methods such as ultrafast 2D NMR, whose quantitative potential has recently been highlighted [17,40].

Acknowledgements

The authors are grateful to Dr. Sabine Bouguet-Bonnet (Univ. Lorraine) for discussions on nOe and spin-diffusion. We also acknowledge Michel Giraudeau for linguistic assistance. This research was supported by funding from the “Agence Nationale de la Recherche” for young researchers (ANR grant 2010-JCJC-0804-01).

Appendix A. Supplementary data

Supplementary material related to this article can be found, in the online version, at http://dx.doi.org/10.1016/j.jpba.2015.01.056.

References

[1] D.J. Cookson, B.E. Smith, Optimal conditions for obtaining quantitative ^{13}C NMR data, J. Magn. Reson. 57 (1984) 355–368.
[2] G.C. Levy, T. Pehk, P.R. Srinivasan, Quantitative ^{15}N NMR spectroscopy, Org. Magn. Reson. 14 (1980) 129–132.
[3] J. Jeener, Lecture Presented at Ampere International Summer School II, Basko Polje, Yugoslavia, 1971.
[4] W.P. Aue, E. Bartholdi, R.R. Ernst, Two-dimensional spectroscopy. Application to nuclear magnetic resonance, J. Chem. Phys. 64 (1976) 2229–2246.
[5] H. Koskela, I. Kilpeläinen, S. Heikkinen, Some aspects of quantitative 2D NMR, J. Magn. Reson. 174 (2005) 237–244.
[6] I.A. Lewis, R.H. Karsten, M.E. Norton, M. Tonelli, W.M. Westler, J.L. Markley, NMR method for measuring carbon-13 isotopic enrichment of metabolites in complex solutions, Anal. Chem. 82 (2010) 4558–4563.
[7] I.A. Lewis, S.C. Schommer, B. Hodis, K.A. Robb, M. Tonelli, W. Westler, M. Sussman, J.L. Markley, Method for determining molar concentrations of metabolites in complex solutions from two-dimensional ^{1}H–^{13}C NMR spectra, Anal. Chem. 79 (2007) 9385–9390.
[8] E. Martineau, P. Giraudeau, I. Tea, S. Akoka, Fast and precise quantitative analysis of metabolic mixtures by 2D ^{1}H INADEQUATE NMR, J. Pharm. Biomed. Anal. 54 (2011) 252–257.
[9] S. Massou, C. Nicolas, F. Letisse, J.-C. Portais, NMR-based fluoxomics: quantitative 2D NMR methods for isotopomers analysis, Phytochemistry 68 (2007) 2330–2340.
[10] E. Martineau, I. Tea, S. Akoka, P. Giraudeau, Absolute quantification of metabolites in breast cancer cell extracts by quantitative 2D ^{1}H INADEQUATE NMR, NMR Biomed. 25 (2012) 985–992.
[11] P. Giraudeau, Quantitative 2D liquid-state NMR, Magn. Reson. Chem. 52 (2014) 259–272.
[12] M. Pathan, S. Akoka, I. Tea, B. Charrier, P. Giraudeau, Multi-scan single shot quantitative 2D NMR: a valuable alternative to fast conventional quantitative 2D NMR, Analyst 136 (2011) 3157–3163.
[13] P. Giraudeau, N. Guignard, E. Hillion, E. Baguet, S. Akoka, Optimization of homonuclear 2D NMR for fast quantitative analysis: application to tropine-nortropine mixtures, J. Pharm. Biomed. Anal. 43 (2007) 1243–1248.

[14] D. Jeannerat, Computer optimized spectral aliasing in the indirect dimension of ^{1}H–^{13}C heteronuclear 2D NMR experiments. A new algorithm and examples of applications to small molecules, J. Magn. Reson. 186 (2007) 112–122.
[15] K. Bingol, F. Zhang, L. Brüschweiler-Li, R. Brüschweiler, Quantitative analysis of metabolic mixtures by two-dimensional ^{13}C constant-time TOCSY NMR spectroscopy, Anal. Chem. 85 (2013) 6414–6420.
[16] R. Brüschweiler, F. Zhang, Covariance nuclear magnetic resonance spectroscopy, J. Chem. Phys. 120 (2004) 5253–5260.
[17] A. Le Guennec, I. Tea, I. Antheaume, E. Martineau, B. Charrier, M. Pathan, S. Akoka, P. Giraudeau, Fast determination of absolute metabolite concentrations by spatially-encoded 2D NMR: application to breast cancer cell extracts, Anal. Chem. 84 (2012) 10831–10837.
[18] H. Koskela, O. Heikkilä, I. Kilpeläinen, S. Heikkinen, Quantitative two-dimensional HSQC experiment for high magnetic field NMR spectrometers, J. Magn. Reson. 202 (2010) 24–33.
[19] R.K. Rai, P. Tripathi, N. Sinha, Quantification of metabolites from two-dimensional nuclear magnetic resonance spectroscopy: application to human urine samples, Anal. Chem. 81 (2009) 10232–10238.
[20] G.A.N. Gowda, F. Tayyari, T. Ye, Y. Suryani, S. Wei, N. Shanaiah, D. Raftery, Quantitative analysis of blood plasma metabolites using isotope enhanced NMR methods, Anal. Chem. 82 (2010) 8983–8990.
[21] W. Gronwald, M.S. Klein, H. Kaspar, S.R. Fagerer, N. Nurnberger, K. Dettmer, T. Bertsch, P.J. Oefner, Urinary metabolite quantification employing 2D NMR spectroscopy, Anal. Chem. 80 (2008) 9288–9297.
[22] P. Giraudeau, I. Tea, G.S. Remaud, S. Akoka, Reference and normalization methods: essential tools for the intercomparison of NMR spectra, J. Pharm. Biomed. Anal. 93 (2014) 3–16.
[23] M. Rajabzadeh, Determination of unknown concentrations of sodium acetate using the method of standard addition and proton nmr: an experiment for the undergraduate analytical chemistry laboratory, J. Chem. Educ. 89 (2012) 1454–1457.
[24] S. Dumitriu, Polysaccharides: Structural Diversity and Functional Versatility, 2nd ed., CRC Press, New York, 2004.
[25] M.M. Fiume, B.A. Heldreth, Scientific literature review on microbial polysaccharides, Cosmet. Ingred. Rev. (2011) 1–52.
[26] V. Popa, Polysaccharides in Medicinal and Pharmaceutical Applications, Smithers Rapra, Shrewsbury, 2011.
[27] S. Mizrahy, D. Peer, Polysaccharides as building blocks for nanotherapeutics, Chem. Soc. Rev. 41 (2012) 2623–2640.
[28] H.J. Jennings, P.A. Pon, Polysaccharides and conjugates as human vaccines, in: S. Dumitriu (Ed.), Polysaccharides in Medical Applications, Marcel Dekker, New York, 1996, pp. 443–479.
[29] D.A. Keire, L.F. Buhse, A. Al-Hakim, Characterization of currently marketed heparin products: composition analysis by 2D-NMR, Anal. Methods 5 (2013) 2984–2994.
[30] G.L. Sassaki, M. Guerrini, R.V. Serrato, A.P. Santana Filho, J. Carlotto, F. Simas-Tosin, T.R. Cipriani, M. Iacomini, G. Torri, P.A.J. Gorin, Monosaccharide composition of glycans based on Q-HSQC NMR, Carbohydr. Polym. 104 (2014) 34–41.
[31] R.M. Crisel, R.S. Baker, D.E. Dorman, Capsular polymer of Haemophilus influenzae, type b. I. Structural characterization of the capsular polymer of strain Eagan, J. Biol. Chem. 250 (1975) 4926–4930.
[32] X. Lemercinier, C. Jones, An NMR spectroscopic identity test for the control of the capsular polysaccharide from *haemophilus influenzae* type b, Biologicals 28 (2000) 175–183.
[33] N. Ravenscroft, G. Averani, A. Bartoloni, S. Berti, M. Bigio, V. Carinci, P. Costantino, S. D'Ascenzi, A. Giannozzi, F. Norelli, C. Pennatini, D. Proietti, C. Ceccarini, P. Cescutti, Size determination of bacterial capsular oligosaccharides used to prepare conjugate vaccines, Vaccine 17 (1999) 2802–2816.
[34] A.J. D'Ambra, J.E. Baugher, P.E. Concannon, R.A. Pon, F. Michon, Direct and indirect methods for molar-mass analysis of fragments of the capsular polysaccharide of haemophilus influenzae type b, Anal. Biochem. 250 (1997) 228–236.
[35] W. Egan, R. Schneerson, K. Werner, Structural studies and chemistry of bacterial capsular polysaccharides. Investigations of phosphodiester-linked capsular polysaccharides isolated from Haemophilus influenzae types a, b, c, and f: NMR spectroscopic identification and chemical modification of end groups and the nature of base-catalyzed hydrolytic depolymerization, J. Am. Chem. Soc. 104 (1982) 2898–2910.
[36] S. Massou, C. Nicolas, F. Letisse, J.-C. Portais, Application of 2D-TOCSY NMR to the measurement of specific ^{13}C-enrichments in complex mixtures of ^{13}C-labeled metabolites, Metab. Eng. 9 (2007) 252–257.
[37] E. Martineau, S. Akoka, R. Boisseau, B. Delanoue, P. Giraudeau, Fast quantitative ^{1}H–^{13}C 2D NMR with very high precision, Anal. Chem. 85 (2013) 4777–4783.
[38] G.N. Manjunatha Reddy, S. Caldarelli, Demixing of severely overlapping NMR spectra through multiple quantum NMR, Anal. Chem. 82 (2010) 3266–3269.
[39] J. Keeler, Understanding NMR Spectroscopy, 2nd ed., John Wiley & Sons, Cambridge, 2010, pp. 285.
[40] P. Giraudeau, L. Frydman, Ultrafast 2D NMR: an emerging tool in analytical spectroscopy, Ann. Rev. Anal. Chem. 7 (2014) 129–161.